Variation of Clumping Index With Zenith Angle for Forest Canopies

Jun Geng, Lili Tu, Jing Chen, Jean-Louis C. H. Roujean, Gang Yuan, Ronghai Hu, Jianwei Huang, Chunju Zhang, Zhourun Ye, Xiaochuan Qu, et al.

Variation of clumping index with zenith angle for forest canopies

Jun Geng, Lili Tu, Jing M. Chen, *Senior Member*, *IEEE*, Jean-Louis Roujean, Gang Yuan, Ronghai Hu, Jianwei Huang, *Member, IEEE,* Chunju Zhang, Zhourun Ye, Xiaochuan Qu, Min Yu, Yongchao Zhu and Qingjiu Tian

***Abstract*—Canopy clumping index (CI) characterizes the extent of the nonrandom spatial distribution of foliage elements within a canopy and is critical for determining the radiative transfer, photosynthesis, and transpiration processes in the canopy. It is widely perceived that CI increases with zenith angle (θ), because between-crown gaps decrease in size and number with increasing θ. In this study, we demonstrate that this is not always true. Analytical equations between CI and θ are first developed based on widely-used forest canopy gap fraction theories. The results show that the zenith angular variation of CI is closely related to crown projected area or crown shapes (i.e., the ratio of the crown height to its diameter, RHD): CI increases with θ for canopies with "tower" crowns (RHD > 1), but decreases with θ for "umbrella" crowns (RHD < 1) and does not vary much with θ for "sphere" crowns (RHD = 1). These results are validated in a LargE-Scale remote sensing data and image Simulation framework (LESS) platform, and published datasets including the measurements in field and RAMI forest stands. The findings are essential for the derivation of angular integrated (hemispherical) CI from *in-situ* measurements and multi-angular remote sensing.**

***Index Terms*—Clumping index, zenith angle, crown shape, ratio of crown height to diameter, angular variation**

Manuscript received July 21, 2022. This work was funded by National Natural Science Foundation of China, grant number 41801234 and 41701383; Anhui Provincial Natural Science Foundation, grant number 2208085MD90 and 2108085QD176; the Fundamental Research Funds for the Central Universities, grant number JZ2022HGTB0253 and JZ2022HGTB0358 (Corresponding author: Lili Tu. & J. M. Chen)

J. Geng, G. Yuan, J. Huang, C. Zhang, Z. Ye, X. Qu, M. Yu, and Y. Zhu are with the School of Civil Engineering, Hefei University of Technology, Hefei 230009, China, and also with the Intelligent Interconnected Systems Laboratory of Anhui Province, Hefei University of Technology, (e-mail: gengj@hfut.edu.cn; 2020110660@mail.hfut.edu.cn; hjw1028@126.com; zcjtwz@sina.com; yezhourun329@hotmail.com; 2004800117@hfut.edu.cn; qqxxcc@hotmail.com; yczhu@hfut.edu.cn)

L. Tu is with the School of Resources and Environment, Anhui Agricultural University, Hefei 230009, China (e-mail: tulili@ahau.edu.cn).

J. M. Chen is with the Department of Geography and Program in Planning, University of Toronto, Toronto, ON M5S 3G3, Canada. He is also with Fujian Normal University, Fuzhou 350000, China. (e-mail: jing.chen@utoronto.ca).

J. Roujean is with with the Centre d'Etudes Spatiales de la Biosphere, University of Toulouse, 31062 Toulouse, France (e-mail: jean-louis.roujean@univ-tlse3.fr).

Ronghai Hu is with the College of Resources and Environment, University of Chinese Academy of Sciences, Beijing 100049, China, and also with the Beijing Yanshan Earth Critical Zone National Research Station, University of Chinese Academy of Sciences, Beijing 101408, China (e-mail: huronghai@ucas.edu.cn).

Q. Tian is with the Jiangsu Provincial Key Laboratory of Geographic Information Science and Technology, International Institute for Earth System Science, Nanjing University, Nanjing, 210046, China (e-mail: tianqj@nju.edu.cn).

I. INTRODUCTION

Forests generally have a high degree of natural variability and typically exhibit complex levels of organization, such as crowns, that cause their foliage to be grouped or clumped [1]. Clumping index (CI) is defined as the ratio of the effective leaf area index (LAI) to the true LAI, and quantifies the degree of deviation of the leaf spatial distribution from the random case (i.e., the Poisson model) [2], [3]. CI is of great significance in terrestrial carbon and water cycle studies as it determines radiation absorption and distribution within plant canopies. CI is closely linked to canopy gap fraction (GF) from which the ratio of sunlit LAI to shaded LAI can be calculated [2]. For a canopy with a random distribution of leaves, the relationship between canopy GF and LAI can be described with the well-known Beer–Lambert theory [4]:

$$P_{Poisson}(\theta)=e^{-LG(\theta)/\cos\theta} \tag{1}$$

where, $P_{Poisson}(\theta)$ is the probability of the transmission of a beam of light at the zenith angle θ through the canopy,i.e., the canopy GF; $G(\theta)$ is the extinction coefficient, which is 0.5 for canopies with a spherical distribution of leaf angles; and L is the LAI, which is most commonly defined as one half the total (all-sided) leaf area per unit ground surface area [5], [6]. As leaves often have nonrandom distributions in reality, i.e., they often aggregate in crowns in forests, CI was first introduced in the modified Beer–Lambert theory for calculating canopy GF by Nilson [4]:

$$P(\theta)=e^{-L\Omega G(\theta)/\cos\theta} \tag{2}$$

where $P(\theta)$ is canopy GF. $\Omega(\theta)$ expresses the zenith angule dependence of the CI [1]. Combining (1) and (2), we can obtain [7]:

$$\Omega(\theta)=\frac{\log[P(\theta)]}{\log[P_{Poisson}(\theta)]} \tag{3}$$

For canopies with randomly distributed leaves, $\Omega = 1$; for most forest canopies, it is found that $\Omega < 1$ because foliage elements usually aggregate within a crown. There exist also rare cases for which $\Omega > 1$, corresponding to canopies with regularly placed leaves. The more clumped a canopy is, the larger the value of canopy GF and the lower the CI value.

The zenith angular variation of CI in *in-situ* measurements has long been recognized in previous studies [1], [8], [9], [10], [11]. As large gaps between foliage clumps (such as crowns) decrease with increasing zenith angle, CI has been found to increase with zenith angle for boreal forests [1], [12], [13],

temperate forests [1], [14], [15], [16], grassland [17], and crops [8], [18], [19], indicating that leaves appear to be more randomly distributed in canopies at larger zenith angles. Recently, based on the sigmoid models [20], sine models [21], and simple linear models [8], [9], the zenith angular variations of CI can be derived from the nadir CI ($\Omega(0)$) [1]. Recently, it was demonstrated that CI can be retrieved from multiple angular remote sensing data at regional and the global scales [7], [22], [23], [24], [25], [26]. The proposed remotely-sensed CI products integrate $\Omega(\theta)$ over the hemispherical space, which is thus independent of the zenith angle [7]. Nonetheless, CI is often dependent on certain directions. Therefore, CI retrievals from remote sensing images need to be transformed first in certain directions prior estimating LAI and particularly sunlit LAI. In the remainder of the paper, CI is considered instead of $\Omega(\theta)$, which is more appropriate with remote sensing techniques in terms of retrievals but which is out of the scope of this study.

Previous studies dealing with CI variations with zenith angle for forest canopies were based on local measurements for specific tree species [1, 7]. These studies established that CI increases with increasing zenith angle in forests for most cases. This study proposed a mathematical expression describing the underlying causes of zenith angular CI variations based on widely-used theories of forest canopy gap fraction. The objective is to derive formulations between CI and zenith angle that are independent of specific tree species and could be applicable for different types of forests.

II. THEORY

CI is closely related to canopy GF (see formula (3)). Therefore, its parameterization relies to a large extent on forest canopy GF theory. The relationship between CI and zenith angle can be considered equivalent to the relationships relating CI and with parameters associated with the zenith angle.

A. Variation of forest canopy GF with zenith angle

Tree distribution in a forest stand is divided into two types: (1) random tree distribution and (2) nonrandom tree distribution.

(1) Random tree distribution

Based on the randomness of natural resources, e.g., water and soil nutrients, a random tree distribution of stems was most of the time considered for forest canopies (especially for natural forests) when considering GF and reflectance models during the last thirty years [27], [28], [29], [30], [31]. This led to use of the binomial distribution for which GF for a forest canopy at nadir for opaque crowns can be expressed as [31], [32],

$$P=\left(1-\frac{t_a}{S}\right)^n \tag{5}$$

where, P is the canopy GF at nadir, S is the forest stand area, t_a is an individual crown projection area in the nadir direction, and n is the crown number. Assuming an isotropic azimuthal distribution of leafy material, directional forest canopy GF without considering gaps within crowns can be expressed as follows [33], [34], [35],

$$P(\theta)=\left(1-\frac{t_a(\theta)}{S(\theta)}\right)^n \tag{6}$$

where, $t_a(\theta)$ and $S(\theta)$ are the crown and forest stand ground projection areas in the direction θ, respectively. The former can be calculated as the geometry, for example, the projection of a ellipsoid crown in the principal plane is a ellipse with a fixed radius r (which is equal to the crown radius) and a height h varying with the view zenith angle θ. The distance between the highest tangent line and the lowest tanglent line of the ellipsoid crown in the view direction is the height of ellipse h. Then, $t_a(\theta)$, which is the area of the ellipse, can be calculated as $[r\cdot h\cdot\pi/2]$. For calculation $t_a(\theta)$ of cone or cylinder crowns, please refer to [35]. Note that $S(\theta)$ turns to $[S\cdot\cos(\theta)]$ for horizontal grounds. If the crown number (n) is sufficiently large, then the binomial distribution becomes the Poisson model, Viz

$$P(\theta)=e^{\frac{-n\cdot t_a(\theta)}{S(\theta)}} \tag{6}$$

For translucent crowns characterized by low LAI values, it is required to consider a different GF for each individual crown. The canopy GF with the random tree distribution reads [31], [35],

$$P(\theta)=\left\{1-\frac{t_a(\theta)\cdot\left[1-P_{gap}(\theta)\right]}{S(\theta)}\right\}^n \tag{7}$$

where $P_{gap}(\theta)$ is the GF of an individual tree crown in the direction θ. It is closely related to the crown projection area ($t_a(\theta)$), the leaf area in an individual crown (L_c), and the leaf inclination projection function ($G(\theta)$). $P_{gap}(\theta)$ can be expressed as follows [31], [35]:

$$P_{gap}(\theta)=e^{-G(\theta)\cdot L_c/t_a(\theta)} \tag{9}$$

For a forest stand with sufficient crowns, then formula (8) resembles to the Poisson model. Combing with formula (7), the variation of canopy GF with zenith angle for a random tree distribution can be expressed as follows:

$$P(\theta)=e^{-n\cdot t_a(\theta)\cdot\left(1-e^{-G(\theta)\cdot L_c/t_a(\theta)}\right)/(S(\theta))} \tag{9}$$

(2) Nonrandom tree distribution

Considering some deviations in *in-situ* measurements from the random case, a robust canopy GF model was presented by Nilson (1999) using a Fisher's group index to describe the tree distribution parameter [31],

$$P(\theta)=e^{[-(1-P_{gap}(\theta))\cdot c_B\cdot C_{CR}\cdot K(\theta)]} \tag{10}$$

where $K(\theta)$ describes the relative change of projection area along with a change in the view direction θ and thus characterizes the crown form. C_{CR} is the crown closure, and can be calculated as the product of the tree projection area at nadir and the stand density ($C_{CR}= t_a(0)\ n/S$). c_B is the tree distribution parameter, which is only related to the Fisher's grouping index GI. (c_B = (-lnGI/ (1-GI)) [31], [37]. For the random tree distribution, $c_B = 1$; trees meet the clumped distribution when $c_B < 1$; trees meet the regular distribution when $c_B > 1$. After considering the nonrandomness of tree distribution and corresponding to the symbol in this study, (9) can be rewritten as follows,

$$P(\theta)=e^{-n\cdot t_a(\theta)\cdot c_B\cdot\left(1-e^{-G(\theta)\cdot L_c/t_a(\theta)}\right)/\left(S(\theta)\right)} \tag{11}$$

B. Variation of CI with zenith angle

Canopy GFs expressed in formula (3) can be transformed in the exponential form. It follows a writing of $\Omega(\theta)$ as,

$$\Omega(\theta)=\frac{n\cdot t_a(\theta)\cdot c_B\cdot\left(1-e^{-G(\theta)\cdot L_c/t_a(\theta)}\right)}{S\cdot G(\theta)\cdot L} \tag{14}$$

It results an expression of the total leaf area as $L_T = S\cdot L = n\cdot L_c$. Then, formula (12) can be written as follows,

$$\Omega(\theta)=\frac{n\cdot c_B}{L_T}\frac{t_a(\theta)}{G(\theta)}\left[1-e^{-\frac{L_T G(\theta)}{n\cdot t_a(\theta)}}\right] \tag{13}$$

Here, the leaf angle distribution (LAD) is classified into spherical and non-spherical as follows:

1) LAD is spherical

In this case, the only parameter associated with the zenith angle in the above equation is the crown projection area $t_a(\theta)$

After gathering some parameters in formula (13), we obtain the coefficient $c_1=\frac{nc_B}{G(\theta)\cdot L_T}=\frac{2nc_B}{L_T}$, which then becomes a constant for a given forest stand, and being independent of the zenith angle. Then, formula (13) can be transformed to the following

$$\Omega(\theta)=c_1\cdot t_a(\theta)\cdot\left[1-e^{\frac{-1}{c_1\cdot t_a(\theta)}}\right] \tag{14}$$

The derivation of (14) with respect to $t_a(\theta)$ (rather than θ) can be expressed as follows,

$$\Omega(t_a(\theta))'=c_1\cdot\left[1-\left(1+\frac{1}{c_1\cdot t_a(\theta)}\right)\cdot e^{\frac{-1}{c_1\cdot t_a(\theta)}}\right]d(t_a(\theta)) \tag{15}$$

We focus on the item of $\left[1-\left(1+\frac{1}{c_1\cdot t_a(\theta)}\right)\cdot e^{\frac{-1}{c_1\cdot t_a(\theta)}}\right]$, and set $t=[c_1\cdot t_a(\theta)]^{-1}$ and this item can be expressed as $f(t)=e^{-t}\left[e^t-(1+t)\right]$. Then, we focus on the item $\left[e^t-(1+t)\right]$, and set

$$g(t)=e^t-(1+t) \tag{16}$$

and derivative of g(t) relative to t is,

$$g(t)'=e^t-1 \tag{17}$$

The $g(t)'$ is always larger than 0. $g(t)$ in (16) has the following two properties:

(1) $g(t)$ is a monotonically increasing function;

(2) $g(t)$ is always greater than 0, because the minimum value of $g(t)$ is $g(0)$.

Then, we draw a conclusion that $f(t)$ and $\Omega(t_a(\theta))'$ are always greater than 0. It indicates that the crown projection area ($t_a(\theta)$) in the direction θ, which is the only parameter related to θ, increases with increasing $\Omega(\theta)$. Therefore, in this case, the relationship between $\Omega(\theta)$ and θ can be transformed to the relationship between $t_a(\theta)$ and θ in this case. In other words, the zenith angular variation of the crown projection area ($t_a(\theta)$) or crown shape plays a key role in the variation of $\Omega(\theta)$ with θ. The relationship between $\Omega(0)$ and $\Omega(\theta)$ is closely related to the crown shape (i.e., $t_a(\theta)$).

Moreover, according to (14), if $\Omega(0)$, $t_a(0)$, and $t_a(\theta)$ are known, c_1 can be solved from an arrangement of (14), and $\Omega(\theta)$ can be calculated without consideration of LAI or L_T.

$$\Omega(0)=c_1\cdot t_a(0)\cdot\left[1-e^{\frac{-1}{c_1\cdot t_a(0)}}\right] \tag{18}$$

2) LAD is non-spherical

If the LAD is non-spherical, we have $c_2=\frac{nc_B}{L_T}$, $x(\theta)=\frac{t_a(\theta)}{G(\theta)}$. Then, formula (13) can be written as follows,

$$\Omega(\theta)=c_2\cdot x(\theta)\cdot\left[1-e^{\frac{-1}{c_2\cdot x(\theta)}}\right] \tag{19}$$

Formula (19) is similar to formula (14) in its mathematical form. Similar to formulas (15-17), the relationship between $\Omega(\theta)$ and θ can be transformed to the relationship between $x(\theta)$ and θ in this case. From the above derivations, the equations for the relationship between CI and zenith angle are first built (see (18) and (19)). The only two parameters are related with zenith angle: a crown projection area ($t_a(\theta)$) and $x(\theta)$ which are determined by the crown shape and LAD (or $G(\theta)$), respectively. The next section will show the influence of these two parameters on the zenith angular variation of CI.

III. RESULTS

Ellipsoids are commonly used to describe crown shape in many forest canopy GF and reflectance models [31], [33], [38], [39], [40]. We use the ratio of crown height to diameter (RHD) to describe various crown shapes. Both the diameter and height of the crown simultaneously change by changing RHD, and crown shape changes from a "tower" shape (crown height is larger than its diameter, i.e., RHD > 1) to an "umbrella" shape (crown height is lower than its diameter, i.e., RHD < 1). Except for the RHD, other structures are set to be the same and within a reasonable range, such as the forest coverage (approximately 53%) and LAI (are equal to 4) are the same in canopies with the three crown shapes (Table I). De Wit (1965) introduced a classification of LAD into four major types, namely planophile (horizontal leaves are most frequent), erectophile (vertical leaves are most frequent), plagiophile (oblique leaves are most frequent), and extremophile (oblique leaves are least frequent) [41]. Other well-known LADs are the uniform (all inclinations are equally frequent) and the spherical distributions (identical to the inclination distribution of the surface elements of a sphere). These six LADs are also adopted in the widely used

TABLE I INPUT PARAMETERS

Parameter	Value
Crown shape	Ellipsoid
Vegetation coverage	53%
LAI	4
Trunk diameter (m)	0.2, **0.3**, 0.5
Trunk height (m)	9, **4.5**, 3.3
Crown radius (m)	0.35, 0.5, 0.7, **1**, 1.41, 2, 2.83
Crown height (m)	16, 8, 4, **2**, 1, 0.5, 0.25
RHD	22.63, 8, 2.83, **1**, 0.35, 0.13, 0.04
Tree density (trees/ha)	19200, 9600, 4800, **2400**, 1200, 600, 300

Bold font means that the crown is a sphere.

SAIL model [42]. Although the LADs are diverse in nature, the above six LADs are commonly-used [41], [43]. The $G(\theta)$ of these six LADs can refer to [44]. As canopy GF directly influences the CI (formula (3)), the zenith angular variations of canopy GFs among different scenes are shown first (Fig. 1).

As the denominators in formula (3) are all the same among different crown shapes in each subplot (only one black line in each subplot (Fig. 1 (a1) - (f1)), the differences among them stem mostly from the difference in the numerators in formula (3). The zenith angular variations of canopy GF show obvious differences among canopies with different RHDs (Fig. 1 (a1) - (f1)). Although the general tendencies of all GFs decrease with increasing zenith angle, the GF decreasing rates are high at low zenith angles but low at high zenith angles for canopies with "tower" crowns. In contrast, the decreasing rates of GF are low at low zenith angles but high at large zenith angles for "umbrella" crowns. According to formula (3), the differences in canopy GF decreasing rates directly lead to different zenith angular variations of CI (Fig. 1 (a2) - (f2)): for canopies with "tower" crowns, CI rapidly increases with increasing zenith

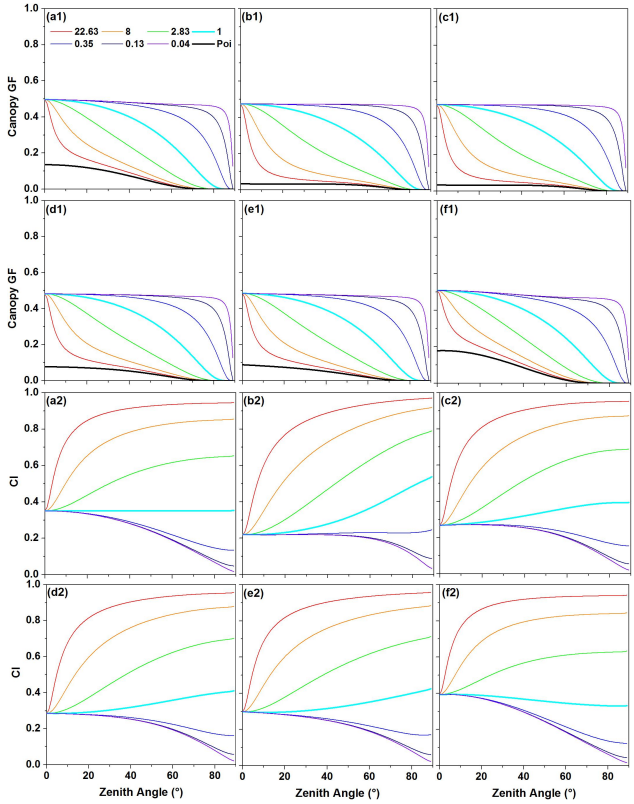

Fig. 1 Relationships between forest canopy GF and CI to zenith angle among different RHDs and LADs. (1: canopy GF, 2: $\Omega(\theta)$; a: spherical, b: planophile, c: plagiophile, d: uniform, e: extremophile, and f: erectophile; Cyan lines mean "sphere" crown; Black lines in the canopy GF subplots indicate the random canopy GF (canopy with leaves meeting the Poisson random distribution; only one black line in each subplot (a1 - f1)); Values in legend (a1) indicate RHD)

angle; in contrast, CI decreases slowly with increasing zenith angle for canopies with "umbrella" crowns. Because of the different RHDs, the change rates of CI differ at various zenith angles: the change rates of CI are large for canopies with "tower" crowns, but low for "umbrella" crowns at low zenith angles. The differences in canopy GF and $\Omega(\theta)$ among canopies with nonspherical LADs show trends similar to those of the spherical LAD (Fig. 1 (a1) and (a2)). Generally, $\Omega(\theta)$ increases with θ for canopies with "tower" crowns, but decreases with θ for "umbrella" crowns. Delineating the influence of LADs on the relationship between $\Omega(\theta)$ and θ is meaningful for the canopies with "sphere" crowns (RHD = 1, cyan lines in Fig. 1). For crowns deviating from the spherical shape (i.e., RHD is obviously larger or lower than 1), the influence of LADs on the relationship between $\Omega(\theta)$ and θ is limited and can be neglected for these typical LADs.

The above results show the influences of RHD and LAD on the zenith angular variations of canopy GF and CI. Here, the influence of the tree distribution is also shown. c_B ranges from 0.85 to 1.77, and forest canopies with the tree distributions ranging from clumped to regular types are given. The crown diameter is 2 m, and its height is 6 m, 2 m, and 1 m, respectively, corresponding to "tower", "sphere", and "umbrella" shapes, respectively. LAI is 4 and LAD is spherical. Overlaps among trees at nadir decrease with increasing values of c_B (see Fig. 2).

The variations of GF and CI with zenith angle are shown in Fig. 3. The influence of tree distribution parameter c_B on both canopy GF and CI are significant. With increasing c_B, canopy GF generally decreases and CI increases for all canopies with three different crown shapes at all zenith angles. Yet c_B does not affect the zenith angular variation of both canopy GF and CI, because it is not related with zenith angle in Nilson's (1999) canopy gap fraction model. For example, CI increases with increasing zenith angle for canopies with "tower" crowns, remains stable for "sphere" crowns, and decreases for "umbrella" crowns.

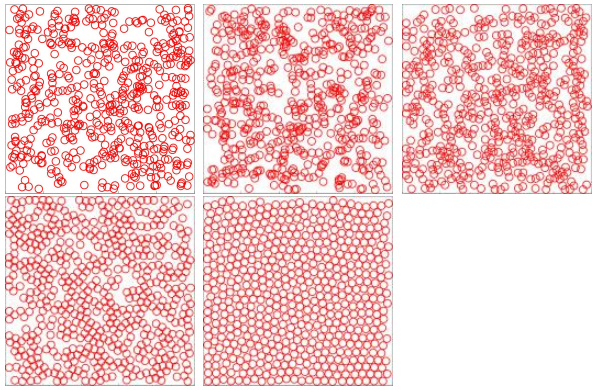

Fig. 2 Forest canopies with different tree distribution parameters (c_B is 0.86, 1.00, 1.20, 1.45, and 1.77, respectively; red circle indicates crown at nadir)

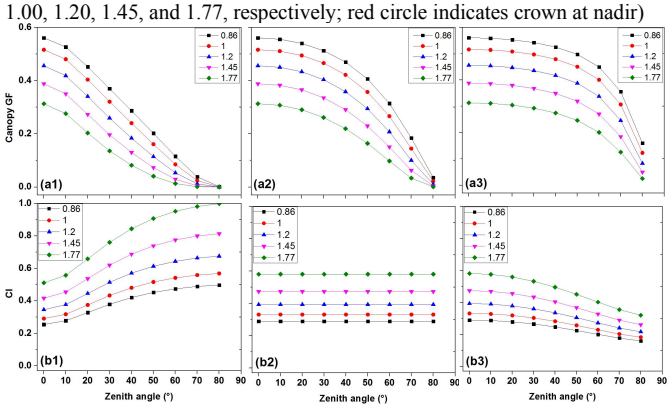

Fig. 3 Zenith angular variation of GF (a) and CI (b) with different tree distributions (1: "tower", 2: "sphere", and 3: "umbrella" shaped. Value in the legend indicates c_B)

IV. VALIDATION

A. Validation in the LESS platform

Two sets of CI measurements are considered as follows: (a) the canopy GF method and (b) the gap size method. In the former, formula (3) is the critical equation in the calculation of CI. The GF of canopies with random leaf spatial distributions (the denominator in formula (3)) is calculated by the well-known Beer–Lambert theory, which has been widely validated and used in many previous studies [4], [31], [45], [46]. Although the forest canopy GF equations appearing in formulas (7-9) have also been widely validated and used in the literature [31], [35], [47], the primary validation exercise focuses on the canopy GF (the numerator in (3)). Then, CI can be directly calculated from the measurements of canopy GF according to formula (3) with a given LAD. The gap size method is the main theory for CI measurements from the Tracing Radiation and Architecture of Canopies (TRAC) instrument. As the large size gaps are the primary reason for the clumping effect, CI can be calculated from a large-gap removal method [2], [3], [48]:

$$\Omega_{CC}(\theta)=\frac{\ln\left[F_m(0,\theta)\right]}{\ln\left[F_{mr}(0,\theta)\right]}\frac{\left[1-F_{mr}(0,\theta)\right]}{\left[1-F_m(0,\theta)\right]} \quad (20)$$

where $F_m(0, \theta)$ is the actual gap-size cumulative distribution function observed along a circular transect in length at zenith angle θ, and F_{mr} $(0, \theta)$ is the reduced gap-size cumulative distribution function after removing the large gaps.

As the canopy GF and gap size decrease with increasing zenith angle in many cases, both essential parameters have low values at large zenith angles, and the discrepancy is attributable to the limited accuracy with which TRAC characterizes small canopy gaps as a result of the penumbra effect. Computer simulation provides a highly controlled environment to implement the validation, and all the confounding factors (e. g., shrub, bush, grass, wind, unstable light conditions, penumbra effect, and complex terrain) affecting the canopy GF and gap size measurements can be explicitly avoided [49]. A 3-D radiative transfer simulation framework LESS (LargE-Scale remote sensing data and image Simulation framework over heterogeneous 3-D scenes: http://lessrt.org) can accurately simulate the canopy GF and the radiation properties of realistic landscapes and has been validated with field measurements. It provides a Python tool to rapidly compute the canopy GF in multiple directions in a batch model [50].

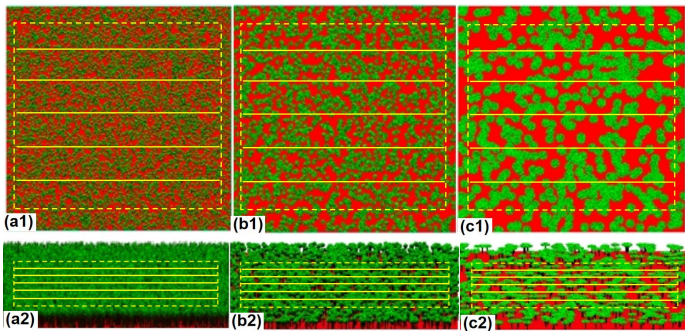

Fig. 4 Three canopy scenes with "tower" (a), "sphere" (b), and "umbrella" crowns (c) in LESS ((1): at nadir; (2) at VZA = 70°. The green regions indicate crowns, and the red region indicate the ground. Yellow lines are the gap size sampling lines which are similar to the trajectories of TRAC; the areas outside of the yellow dashes are not considered to avoid the boundary effect)

Three canopies with "tower", "sphere", and "umbrella" crowns (RHD = 8, 1, and 0.13) are built in LESS (Fig. 4); the LAD is spherical, the LAI ranges from 0.75 to 4, and other parameters are listed in Table I. The scenes in the LESS platform provided good conditions. Unlike digital hemispherical photographs, the canopy GF observations from the top to the bottom with the parallel projection do not need to consider the sampling effect. The boundary effect of the canopy GF is considered, i.e., the regions near the boundary of the stand are not considered, especially for large zenith angles (the areas outside of yellow dashes in Fig. 4 are not considered to avoid the boundary effect). Based on image processing (e.g., image binarization), the whole canopy GF and gap sizes on five equidistant sampling lines can be obtained.

1) Canopy GF method

Essentially, the canopy GF method is based on the definition of CI and formula (3). Here, the primary work focuses on comparing the forest GF between formula (9) (or the numerator in formula (3)) and LESS results at multiple zenith angles. As shown in Fig. 5, the measured canopy GFs are generally consistent with the formula results in this study at most zenith angles, especially at low zenith angles. The root-mean-square errors (RMSEs) in the canopy GF between the measured and formula results are listed in Table II. The maximum value of RMSE is less than 0.07, indicating that canopy GFs calculated with formula (9) are validated. The decreasing rates of GF vary with crown shape: the canopy GFs are stable for canopies with "umbrella" crowns but rapidly decrease for "tower" crowns at low zenith angles; in contrast, they rapidly decrease for "umbrella" crowns, but are stable for "tower" crowns at high zenith angles. As there are different decreasing rates of canopy GF among different crown shapes (e.g., large gaps between crowns are rarely found for "tower" crowns, but are still easily found for "umbrella" crowns at large zenith angles, as shown in Fig. 5. (c2)), the different zenith angular variations of CI are found. CI can be directly calculated from canopy GF with a given LAI (Table I) and LAD (spherical) according to (1) and (3) (Fig. 5 (b)). As canopy GFs are validated in LESS, CIs are also validated. Slight biases in the canopy GF at large zenith

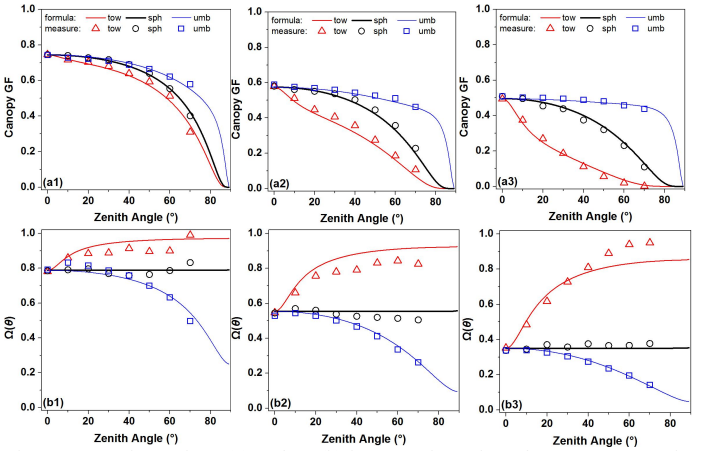

Fig. 5 Comparison of GF (a) and CI (b) between formula and measurement using the GF method ((1) - (3) mean LAI = 0.75, 2, and 4, respectively. "tow", "sph", and "umb" mean canopies with "tower", "sphere", and "umbrella" crowns, respectively)

TABLE II RMSEs OF GF AND CI BETWEEN FORMULA RESULTS AND MEASUREMENTS BASED ON THE GF METHOD

Crown	GF			CI		
	LAI = 0.75	LAI = 2	LAI = 4	LAI = 0.75	LAI = 2	LAI = 4
"tower"	0.064	0.036	0.019	0.048	0.067	0.070
"sphere"	0.009	0.019	0.016	0.022	0.028	0.018
"umbrella"	0.013	0.010	0.010	0.030	0.014	0.007

angles can lead to significant errors in CI because the relationship between the canopy GF and CI is logarithmic. Although there are some deviations in CI between the formula and measurements at large zenith angles, the maximum of RMSE is only 0.070 (Table II). This means that both canopy GF and CI calculations in this study are reliable.

2) Gap size distribution method ($\Omega_{CC}(\theta)$)

Each canopy's gap sizes in five equidistant sampling lines (yellow lines in Fig. 4) at multiple zenith angles are recorded. Fig. 6 clearly shows the gap size distributions along the middle sampling line at multiple zenith angles. Gaps can be divided into two types: gaps within a crown and gaps between crowns. All gaps decrease with increasing LAI, especially for the within-crown gaps. With increasing zenith angle, the within-crown gap size decreases for all canopies. However, the zenith angular variation of between-crown gap size shows completely different variations among these three canopies: for the canopy with "tower" crowns, the gap size decreases quickly with increasing zenith angle (Fig. 6 (a1) - (a3)); while, for the canopies with "sphere" (Fig. 6 (b1) - (b3)) and "umbrella" crowns (Fig. 6 (c1) - (c3)), there is no obvious decrease in between-crowns gap size with increasing zenith angle. Especially for the canopy with "umbrella" crowns, large gap sizes show increasing trends with increasing zenith angle.

The gap size distribution method calculates the CI based on a large-gap removal strategy. Therefore, the distribution of between-crown gaps, which are often large gaps, plays an essential role in the calculation of CI [13]. The different zenith angular variations of gap size distributions in Fig. 6 directly lead to the different zenith angular variations of CI based on the gap size distribution method. After recording the gap size in each sampling line, $\Omega_{CC}(\theta)$ can be calculated using CIMES software in which the gap size distribution method is integrated [51]. In the legend in Fig. 7, "measure" indicates that the CI is calculated with the gap size distribution method in the LESS platform. At large zenith angles (e.g., θ >50°), small gaps are rarely found in the sampling lines for "tower" crowns, and the CI output in CIMES cannot be calculated, leading to the CI value in Fig. 7 being null at large zenith angles.

Although the sampling line increases the randomness of the observations, clearly different trends are shown in Fig. 7 for these three canopy types with different crown shapes. As shown in Fig. 7, there are obviously different variations of CI with zenith angle for forests with all three different crown types: the $\Omega_{CC}(\theta)$ strongly increases with increasing zenith angle for canopies with "tower" crowns, while it shows a slow increasing trend for "sphere" crowns and a downtrend for "umbrella" crowns. The RMSEs of the CI between the formula results and

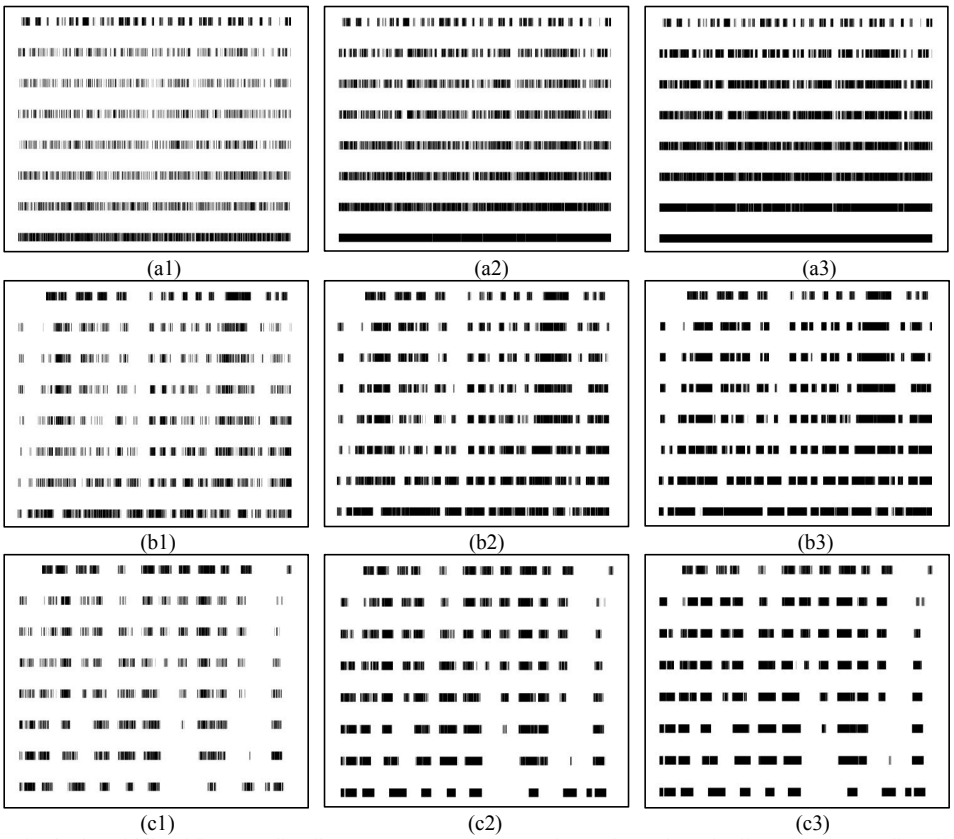

Fig. 6 Comparison of gap size in the middle of five sampling lines among "tower" (a), "sphere" (b), and "umbrella" crowns (c) (8 lines in each subplot record gap size at zenith angle = 0° - 70°, increasing step is 10°. Black rectangles mean leaves and write rectangles among black rectangles mean gaps; (1) - (3) mean LAI = 0.75, 2, and 4, respectively)

the measurements based on the gap size method are listed in Fig. 7. For LAI = 0.75 and 2, the maximum value of the RMSE is lower than 0.1. The relatively large differences between the measured $\Omega_{CC}(\theta)$ and formula results appear in canopies with large LAIs at large zenith angles. For large zenith angles (e.g., θ >50°), the overlaps among crowns increase, and the size of the benchmark, in which the leaves meet random distribution and CI is equal to 1 (such as a crown without overlaps in the view direction), also decrease. The termination conditions of the iteration for the gap size distribution method is a key step for calculating CI. The final value of the projected LAI (L_p) in θ direction is found after several iterations of the same steps until no increase in L_p is found, such as the large gaps are removed and small gaps remain. As the overlaps among crowns increase, large gaps among "umbrella" crowns still exist at large zenith angles (see Fig. 4). Significant non-randomness and heterogeneity of the canopy still exist at large zenith angles even though the large gaps among crowns are removed. Therefore, some relatively small gaps among crowns may also need to be removed. While identifying small gap sizes is not

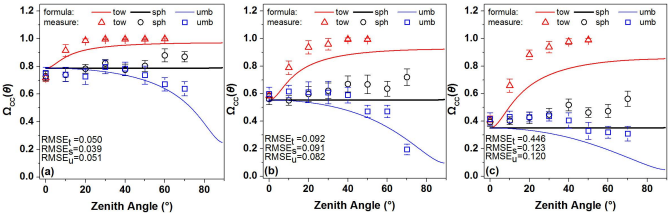

Fig. 7 Comparison of CI between formula and measurement using the gap size method (a-c mean LAI = 0.75, 2, and 4, respectively. "tow", "sph", and "umb" mean canopies with "tower", "sphere", and "umbrella" crowns, respectively).

easy, and these gaps are often rarely recorded when too many overlaps among crowns occur more at larger zenith angles. This is considered the saturation point in the identification of small gap sizes due to too many overlaps among crowns at large zenith angles.

B. Validation based on the published datasets

1) Field measurements datasets in Kucharik *et al.* (1999)

The zenith angular variations of CI field measurements for three tree species (old jack pine (OJP), old black spruce (OBS), and old aspen (OA)) were published in Kucharik *et al.* (1999). Here, we used the same datasets to validate the results in this study. The measurements included the mean crown height (6.5 m, 7 m, and 4.5 m for the three tree species, respectively), crown diameter (1.94 m, 1.38 m, and 3.4 m for the three tree species, respectively), and density (1800, 4480, and 847 stem/ha for the three tree species, respectively). CI(0) was measured by a multiband vegetation imager, and CI(θ) was measured by TRAC. Moreover, based on the assumption that CI increases with increasing zenith angle and is equal to 1 from the horizontal view (θ = 90°), CI(θ) was simulated by the Monte Carlo method in Kucharik *et al* (1999). Here, we extract both the field measured CIs ("Measure" in Fig. 8) and simulated CIs ("K-MC" in Fig. 8) in Kucharik *et al* (1999). LAD is assumed to be uniform. As crown diameter, crown height, tree density, and CI(0) are known, CI(θ) can be calculated based on formula (19) ("Formula" in Fig. 8).

Although CIs increase with increasing zenith angle for the three tree species in "Formula", "K-MC" and "Measure", their increasing rates are different. CI shows obviously slow growth for the OA stand. The CI values of "Measure" for the OA stand tend to be saturated at θ > 40°. Generally, the CI increasing rates captured by the "Formula" in this study show better consistency with the measured CI than those captured by the "K-MC", especially at large zenith angles. The RMSE in CI(θ) between "Formula" and "Measure" is only 0.027, 0.064, and 0.061, respectively, for the three tree species. However, the RMSE in CI(θ) between "K-MC" and "Measure" is 0.076, 0.071, and 0.126 for the three tree species, respectively. The main differences in CI(θ) between "K-MC" and "Measure" appear at the large zenith angles, especially for the OA stand. The assumption that CI increases with increasing zenith angle is responsible for the RMSE in CI(θ) between "K-MC" and "Measure", especially for the OA stand.

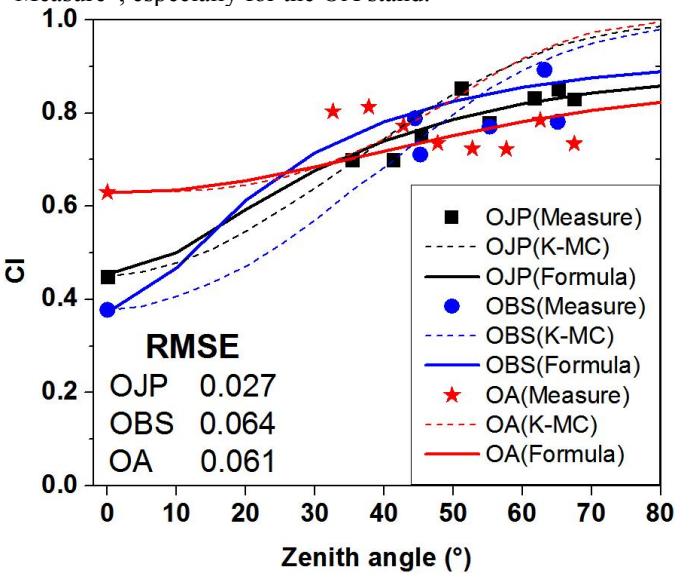

Fig. 8 Validation of CI(θ) in this study used the filed measurements ("Measure" indicates CI(θ) in the *in-situ* measurements; "K-MC" indicates CI(θ) simulated by the Monte Carlo based on the assumption that CI increases with increasing θ and is equal to 1 from the horizontal view; "Formula" indicates CI(θ) calculated in this study; "RMSE" is the RMSE in CI(θ) between "Formula" and "Measure"; "Measure" and "K-MC" results are derived from Kucharik *et al.* (1999))

2) RAMI stand-level datasets in Hu *et al.* (2014)

Two HET-04 forest stands with "cylinder" shaped (crown height is 12 m, and its diameter is 3 m, similar to "tower" shaped) and "sphere" shaped crowns (crown diameter is 4 m) are given in the RAdiative transfer Model Intercomparison exercise (RAMI) platform in Hu *et al.* (2014) [11]. LADs for these two forest canopies are uniform. For detailed information on the forest structures (e.g., LAI, tree density, crown height and diameter) of these two forest stands, please refer to Hu *et al.* (2014) and the RAMI website. Tree positions are shown in Fig. 9, indicating that overlaps among trees are rare. The tree distribution parameter c_B is calculated according to Nilson (1999). c_B for the forests with "cylinder" crowns and "sphere" crowns are 1.03 and 1.20, respectively. There are no forest stands with "umbrella" crowns in the RAMI platform. Keeping the tree positions and crown diameter unchanged, the crown height is one half of the "sphere" crown diameter. Then, a forest stand with "umbrella" crowns is built based on the RAMI HET-04 stand with "sphere" crowns.

For forest canopies with "cylinder" crowns and "sphere" crowns, the effective LAIs were measured in Hu *et al.* (2014).

Then, CI(θ) can be directly calculated by the definition of CI because LAIs are given in the RAMI HET-04 stand. For forest canopies with "umbrella" crowns, the zenith angular variation of canopy GF can be measured based on the image processing method. Then, CI(θ) can be obtained based on formula (3).

The CI calculated by formula (19) in this study and the measurements in Hu *et al.* (2014) for these three different crown shapes are shown in Fig. 10. The zenith angular variations of CIs are obviously different among these three forests with different crown shapes. The "formula" CI(θ) curves in Fig. 10 are highly consistent with the RAMI measurements in Hu *et al.* (2014). The RMSE in CI(θ) between "Formula" and "RAMI" is only 0.031, 0.032, and 0.029, respectively, indicating that the formula results in this study are validated. Therefore, it is reasonable to believe that the assumption in Kucharik *et al.* (1999) that CI increases with increasing zenith angle may be not always true and is limited to "tower" crown shapes.

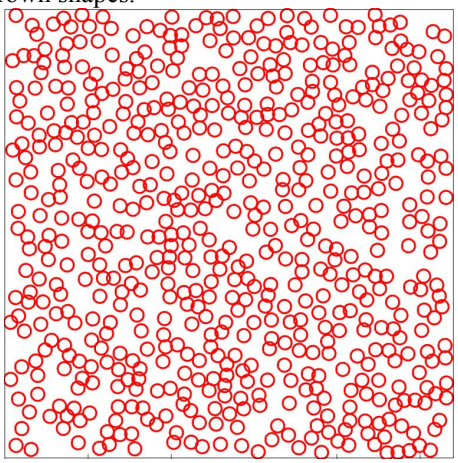

Fig. 9 Tree positions in the RAMI HET-04 forest stand (red circles indicate crowns at nadir)

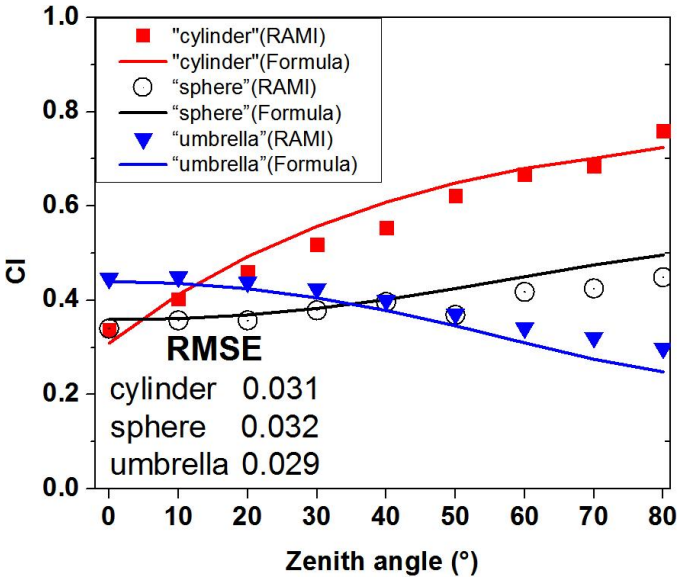

Fig. 10 Validation of CI(θ) in this study using the RAMI HET-04 measurements ("RMSE" is the RMSE in CI(θ) between "Formula" and "RAMI";"RAMI" CI of forest canopies with "cylinder" and "sphere" crowns are derived from Hu *et al.* (2014))

V. Discussions

With the presence of crowns, leaves often show significant clumping effects rather than random or regular effects in the forest canopies. Previous studies often reported that this aggregated effect was more obvious at low zenith angles than that at large zenith angles because the large gaps between crowns could be more easily found at low zenith angles. The relationships between CI and zenith angle for canopies with "tower" crowns in this study are consistent with previous studies: CI increases with increasing zenith angle. For canopies with "sphere" and "umbrella" crowns, the results in this study show different angular patterns from those in many previous studies. For "sphere" crowns with the spherical LAD, both the crown projection (t_a) and crown GF (P_{gap}) are independent of the zenith angle. As crowns are randomly distributed in a region, crown CI (quantifying the degree of deviation of the crown (rather than leaf) spatial distribution from the random case) is always equal to 1 and independent of the zenith angle. Therefore, it is easily understood that CI does not vary with zenith angle for "sphere" crowns with the spherical LAD. Compared with the "sphere" crowns, canopies with "umbrella" crowns produce a larger canopy GF at larger zenith angles, leading to a lower CI. Similarly, the zenith angular variation of the CI with "tower" crowns can also be clearly explained. All tree diameters are lower than their heights in field measurements in Kucharik *et al*. (1999), indicating that all tree crowns are "tower" shaped [1]. The results in Kucharik *et al*. (1999) showed that CI increased with increasing zenith angle, which is partly consistent with the forests with "tower" crowns in this study. While, based on the assumption that CI always increases with increasing zenith angle, the first equation between CI and zenith angle was developed by Kucharik *et al*. (1999). In the equation, CI(θ) can be calculated from CI(0) using tree species-specific semi-empirical parameters. The results of this study show this assumption in Kucharik *et al*. (1999) that CI always increases with increasing zenith angle is valid only for canopies with "tower" crowns. We derived a new equation in this study, which presents a different viewpoint on the zenith angular variation of CI: CI may not always increase with increasing zenith angle. It mainly depends on the crown RHD. This new viewpoint is supported by the field measurements in Hu *et al*. (2012).

The results in this study show that the zenith angular variation of CI is affected by both crown shape and LAD. The averaged leaf inclination angle in the six well-known LADs used in this study ranges from 26.8° to 63.2°, which cover the most cases of leaf inclination angles for forests. For forest canopies with extreme LADs, such as the averaged leaf inclination angle lower than 26.8° or larger than 63.2°, formula (19) is suggested to be most suitable for describing the zenith angular variation of CI. Although LAD affects the zenith angular variation of CI, the influence may be limited (Fig. 1). This is reasonable because LAD is the inclination distribution of leaves, yet CI describes the spatial distribution of leaves. LAD and leaf spatial distribution are two independent parameters according to their definitions in theory. Moreover, tree crowns show various shapes (i.e., crown RHD in this study)

at the global scale. As the annual mean solar zenith angle increases from the equator to high latitudes, crowns with different height-to-width ratios have inherently varying efficiencies of light interception, e.g., the dominance of tall and thin conifers at high latitudes, and flat-topped trees at low latitudes. Therefore, we suggest that main attention should be paid to crown shape when the zenith angular variation of CI is studied. Previous studies about the zenith angular variation of CI have all focused on forest canopies with "tower" crowns, leading to the widely accepted perception that CI always increases with increasing zenith angle. The results in this study show a new viewpoint regarding the zenith angular variation of CI, especially for forest canopies with "sphere" and "umbrella" crowns.

The forest canopy GF model considering the tree distributions in Nilson (1999) is robust for many forests. Yet it is not suitable for any forests. An assumption was made in Nilson (1999): forest canopy is azimuthally isotropic and there is no azimuth angle in the whole derivation in Section II. Therefore, the model is unworkable for forest canopies with obvious azimuthal anisotropy, such as orchards in which the tree distributions are obviously grid-shaped and line-shaped. Fang *et al.* (2014) showed a slight decrease in CI with zenith angle for paddy rice fields [9]. The zenith angular variation of CI for grid-shaped and line-shaped forests (e.g., orchards) or crops is due to the large gaps between the crowns or rows at large zenith angles. For these particular tree distributions (grid-shaped and line-shaped), CI varies with not only the zenith angle but also the azimuth angle because of the obvious azimuthal anisotropy of the canopy GF for these vegetation canopies. A similar trend has also been reported for regularly spaced trees, and the relationship between $\Omega(\theta)$ and θ can be described as a sigmoid model [1]. Essentially, the particular zenith angular variations of CI in grid-shaped and line-shaped vegetation canopies are still due to the zenith angular variation of canopy GF. It is our strategy in studying the zenith angular variation of CI: based on the canopy GF theory according to formula (3). We believe that the zenith angular variation of CI is actually due to the zenith angular variation of canopy GF. In addition, the leaves are assumed to be randomly distributed in an individual crown, and the clumping effect within crown is not considered in this study. Formula (18-19) is invalid for forest canopies with obvious branch structures or obviously aggregated structures within crowns. We believe that the zenith angular variation of canopy GF is still a critical task to study the zenith angular variation of CI in these forests.

VI. Conclusion

Clumping index (CI), which is an essential parameter to determine radiation distribution in plant canopies, varies with zenith angle. It is widely accepted that CI increases with increasing zenith angle in the past twenty years. In this study, based on the widely-used forest canopy GF theories, an analytical derivation is performed on the variation of CI with zenith angle for forest canopies. The results show a different viewpoint from the widely-accepted zenith angular variation of CI. Specifically, (1) the crown shape (i.e., the ratio of the crown height to diameter, RDH) is proven to be a key parameter in determining the variation pattern of CI with zenith angle: CI increases with the zenith angle for forest canopies with "tower" crowns (RDH > 1), does not vary much with zenith angle for "sphere" crowns (RHD = 1), and decreases for "umbrella" crowns (RDH < 1). New equations about CI and zenith angle are developed in this study, which would be useful for not only CI *in-situ* measurement but also CI retrieval using remote sensing images.

Acknowledgment

The authors would like to thank Prof. Andres Kuusk, Prof. Guang Zheng, and Dr. Li-xia Ma for the helpful discussions.

Jun Geng received the M.S. degree in ecology from Nanjing Forestry University, Jiangsu, China, in 2012, and the Ph. D degree in geography from Nanjing University, Nanjing, China, 2016. He is a Lecturer with the College of Civil Engineering, Hefei University of Technology, Hefei, China. His research interests include the relationship between canopy structure and BRDF, canopy reflectance modeling, remote sensing modeling and applications for vegetation ecosystem.

Lili Tu received the M.S. degree from Nanjing University, Jiangsu, China, in 2012, and the Ph. D degree in geography from Nanjing University, Nanjing, China, in 2017. She is currently a Lecturer with the School of Resources and Environment, Anhui Agricultural University, China. Her research interests include multi-angle remote sensing, applications for vegetation ecosystem, and the application of thermal infrared remote sensing.

Jing M. Chen (Senior Member, IEEE) received the Ph.D. degree in meteorology from Reading University, Reading, U.K., in 1986. He is a Professor with the Department of Geography and Program in Planning, University of Toronto, Toronto, ON, Canada; a Canada Research Chair; and a Fellow of the Royal Society of Canada. He is also a Professor with Fujian Normal University, Fuzhou, China. He has published over 200 papers in refereed journals, which have been cited over 5000 times in the scientific literature. His major research interests include remote sensing of vegetation and quantifying terrestrial carbon and water fluxes. Dr. Chen is currently an Editor-in-Chief of *Remote Sensing of Environment*, and Associate Editor of *the Journal of Geophysical Research-Atmosphere*, *Canadian Journal of Remote Sensing* and *Journal of Applied Remote Sensing*.

Jean-Louis Roujean received the Ph.D. degree from the University Paul Sabatier, Toulouse, France, in 1991. Then he was a CNES Postdoctoral Fellow at the Centre National de Recherches Météorologiques (CNRM) – the research branch of Météo France - until he joined the Centre National de la Recherche Scientifique (CNRS) in

1994. From 1999 to 2008, he was at the Head of Remote Sensing Group for Land Surface Studies at CNRM. Between 2016 and 2017, he was appointed CNRS adjoined director of CNRM before moving to CESBIO. Then, he was President of TOSCA – a national committee in charge of evaluating spatial activities - for Land Surface group until 2020. He is currently Director of Research at CNRS and published 102 papers in peer-review journals. He has been involved in several Framework Programs of the European Union (FP5/CYCLOPES, FP6/GEOLAND, and FP7/ImagineS), and more recently the Global Land Service of Copernicus. He was responsible for the development and operational implementation of shortwave radiative fluxes products for Meteosat in the frame of the Land Surface Analysis for Satellite Application Facilities project from EUMETSAT. His well known research concerns the modeling of surface bidirectional reflectance distribution function (BRDF) and albedo based on kernel-driven approach. He is the French Principal Investigator of the TRISHNA mission aimed to map the temperature of the Earth at high spatiotemporal resolution from 2025.

Gang Yuan received the B.S. degree in surveying engineering in 2020 from Hefei University of Technology, Anhui, China, where he is currently working toward the M.S. degree in surveying engineering. His research interests include canopy modeling and machine learning.

Ronghai Hu is with the College of Resources and Environment, University of Chinese Academy of Sciences, Beijing 100049, China, and also with the Beijing Yanshan Earth Critical Zone National Research Station, University of Chinese Academy of Sciences, Beijing 101408, China.

Jianwei Huang (Member, IEEE) received the B.S. degree in surveying and mapping engineering and the Ph.D. degree in digital mine engineering from Northeastern University, Shenyang, China, in 2012 and 2019, respectively. He is a Lecturer with the College of Civil Engineering, Hefei University of Technology, Hefei, China. His research interest includes disaster remote sensing.

Chunju Zhang received the Ph.D. degree in cartography and geographic information system from the School of Geographical Science, Nanjing Normal University, Nanjing, China, in 2013. She is an Associate Professor with the School of Civil Engineering, Hefei University of Technology, Hefei, China. Her research interests include computational intelligence in remote sensing images and geographic knowledge graph.

Zhourun Ye was born in Anhui, China. He received the B.S. degree in geomatics engineering from Liaoning Technical University, Liaoning, China, in 2007 and the M.S. and Ph.D. degrees in geodesy and geomatics engineering from the University of Chinese Academy of Sciences, Beijing, China in 2010 and 2015, respectively. He was a Visiting Ph.D. Student with the University of Stuttgart, Stuttgart, Germany, for 24 months, i.e., from November 2012 to October 2014. He is an Associate Professor with the School of Civil Engineering, Hefei University of Technology, Hefei, China.

Xiaochuan Qu is currently a lecturer at the college of civil engineering, Hefei University of Technology. He graduated from Wuhan University and obtained his Ph.D degree in 2014. He is a Lecturer with the College of Civil Engineering, Hefei University of Technology, Hefei, China. His current research interests include GNSS Meteorology, and tropospheric/ionospheric delay modeling.

Min Yu was born in Anhui, China. He received the B.S. degree in Photogrammetry and Remote Sensing, Wuhan Technical University of Surveying and Mapping, in 1999, and M.S. degrees in Photogrammetry and Remote Sensing, Wuhan University, in 2004, Wuhan, China, respectively. He is a Lecturer with the College of Civil Engineering, Hefei University of Technology, Hefei, China. His current research interests include UAV Photogrammetry and modeling.

Yongchao Zhu was born in Hubei, China. He received the B.S. and M.S. degrees in geomatics engineering and the Ph.D. degree in geodesy and geomatics engineering from Wuhan University, Wuhan, China, in 2012, 2014, and 2018, respectively. He was a Visiting Ph.D. Student with German Research Center for Geosciences GFZ for 18 months, i.e., from January 2017 to July 2018. He is currently with the College of Civil Engineering, Hefei University of Technology, China. His research interests include ocean and land remote sensing applications using GNSS-reflectometry techniques.

Qingjiu Tian received the B.S. degree from Shandong University, Shandong, China, in 1987, the M.S. degree from Chinese Academy of Sciences (CAS), Beijing, China, in 1996, and the Ph.D. degree from Nanjing University, Jiangsu, China, in 2003.
He is currently a Professor with the International Institute for Earth System Sciences, Nanjing University, Nanjing, China. His major research interests include retrieval of vegetation parameters from hyper-spectral remote sensing and multi-angular remote sensing data. Dr. Tian is currently an Associate Editor of *National Remote Sensing Bulletin*.

References

[1] C. J. Kucharik, J. M. Norman, and S. T. Gower, "Characterization of radiation regimes in nonrandom forest canopies: theory, measurements, and a simplified modeling approach," *Tree Physiol.*, vol. 19, no. 11, pp. 695-706, 1999-01-01. 1999, doi: 10.1093/treephys/19.11.695.

[2] J. M. Chen and J. Cihlar, "Plant canopy gap-size analysis theory for improving optical measurements of leaf-area index," *Appl. Optics*, vol. 34, no. 27, pp. 6211-6222. 1995.

[3] H. Fang, "Canopy clumping index (CI): A review of methods, characteristics, and applications," *Agric. For. Meteorol.*, vol. 303, p. 108374. 2021, doi: 10.1016/j.agrformet.2021.108374.

[4] T. Nilson, "A theoretical analysis of the frequency of gaps in plant stands," *Agricultural Meteorology*, vol. 8, pp. 25-38. 1971.

[5] J. M. Chen and T. A. Black, "Defining leaf area index for non-flat leaves," *Plant, Cell \& Environment*, vol. 15, no. 4, pp. 421-429. 1992.

[6] G. Zheng and L. M. Moskal, "Retrieving Leaf Area Index (LAI) Using Remote Sensing: Theories, Methods and Sensors," *Sensors*, vol. 9, no. 4, pp. 2719-2745, 2009-01-20. 2009, doi: 10.3390/s90402719.

[7] J. M. Chen, C. H. Menges, and S. G. Leblanc, "Global mapping of foliage clumping index using multi-angular satellite data," *Remote Sens. Environ.*, vol. 97, no. 4, pp. 447-457. 2005, doi: 10.1016/j.rse.2005.05.003.

[8] H. Fang, W. Liu, W. Li, and S. Wei, "Estimation of the directional and whole apparent clumping index (ACI) from indirect optical measurements," *ISPRS-J. Photogramm. Remote Sens.*, vol. 144, pp. 1-13. 2018, doi: 10.1016/j.isprsjprs.2018.06.022.

[9] H. Fang, W. Li, S. Wei, and C. Jiang, "Seasonal variation of leaf area index (LAI) over paddy rice fields in NE China: Intercomparison of destructive sampling, LAI-2200, digital hemispherical photography (DHP), and AccuPAR methods," *Agric. For. Meteorol.*, vol. 198-199, pp. 126-141. 2014, doi: 10.1016/j.agrformet.2014.08.005.

[10] A. Gonsamo and P. Pellikka, "The computation of foliage clumping index using hemispherical photography," *Agric. For. Meteorol.*, vol. 149, no. 10, pp. 1781-1787. 2009, doi: 10.1016/j.agrformet.2009.06.001.

[11] R. Hu, G. Yan, X. Mu, and J. Luo, "Indirect measurement of leaf area index on the basis of path length distribution," *Remote Sens. Environ.*, vol. 155, pp. 239-247. 2014, doi: 10.1016/j.rse.2014.08.032.

[12] S. G. Leblanc, J. M. Chen, H. P. White, R. Latifovic, R. Lacaze, and J. Roujean, "Canada-wide foliage clumping index mapping from multiangular POLDER measurements," *Can. J. Remote Sens.*, vol. 31, no. 5, pp. 364-376. 2005.

[13] J. M. Chen, "Optically-based methods for measuring seasonal variation of leaf area index in boreal conifer stands," *Agric. For. Meteorol.*, vol. 80, no. 2, pp. 135-163. 1996.

[14] J. Zou, G. Yan, and L. Chen, "Estimation of Canopy and Woody Components Clumping Indices at Three Mature Picea crassifolia Forest Stands," *IEEE J. Sel. Top. Appl. Earth Observ. Remote Sens.*, vol. 8, no. 4, pp. 1413-1422. 2015, doi: 10.1109/JSTARS.2015.2418433.

[15] C. Macfarlane *et al.*, "Estimation of leaf area index in eucalypt forest with vertical foliage, using cover and fullframe fisheye photography," *For. Ecol. Manage.*, vol. 242, no. 2-3, pp. 756-763. 2007, doi: 10.1016/j.foreco.2007.02.021.

[16] L. Ma, G. Zheng, X. Wang, S. Li, Y. Lin, and W. Ju, "Retrieving forest canopy clumping index using terrestrial laser scanning data," *Remote Sens. Environ.*, vol. 210, pp. 452-472. 2018, doi: 10.1016/j.rse.2018.03.034.

[17] Y. Nouvellon *et al.*, "PAR extinction in shortgrass ecosystems: effects of clumping, sky conditions and soil albedo," *Agric. For. Meteorol.*, vol. 105, no. 1, pp. 21-41, 2000-01-01. 2000, doi: 10.1016/S0168-1923(00)00194-5.

[18] J. Liu, E. Pattey, and S. Admiral, "Assessment of in situ crop LAI measurement using unidirectional view digital photography," *Agric. For. Meteorol.*, vol. 169, pp. 25-34. 2013, doi: 10.1016/j.agrformet.2012.10.009.

[19] V. E. R. Demarez, S. Duthoit, F. E. D. E. Baret, M. Weiss, and G. E. R. Dedieu, "Estimation of leaf area and clumping indexes of crops with hemispherical photographs," *Agric. For. Meteorol.*, vol. 148, no. 4, pp. 644-655. 2008.

[20] S. Duthoit, V. Demarez, J. Gastellu-Etchegorry, E. Martin, and J. Roujean, "Assessing the effects of the clumping phenomenon on BRDF of a maize crop based on 3D numerical scenes using DART model," *Agric. For. Meteorol.*, vol. 148, no. 8-9, pp. 1341-1352. 2008, doi: 10.1016/j.agrformet.2008.03.011.

[21] F. Montes, P. Pita, A. Rubio, and I. Cañellas, "Leaf area index estimation in mountain even-aged Pinus silvestris L. stands from hemispherical photographs," *Agric. For. Meteorol.*, vol. 145, no. 3-4, pp. 215-228. 2007, doi: 10.1016/j.agrformet.2007.04.017.

[22] Z. Jiao *et al.*, "An algorithm for the retrieval of the clumping index (CI) from the MODIS BRDF product using an adjusted version of the kernel-driven BRDF model," *Remote Sens. Environ.*, vol. 209, pp. 594-611. 2018, doi: 10.1016/j.rse.2018.02.041.

[23] S. Wei and H. Fang, "Estimation of canopy clumping index from MISR and MODIS sensors using the normalized difference hotspot and darkspot (NDHD) method: The influence of BRDF models and solar zenith angle," *Remote Sens. Environ.*, vol. 187, pp. 476-491. 2016, doi: 10.1016/j.rse.2016.10.039.

[24] L. He *et al.*, "Inter- and intra-annual variations of clumping index derived from the MODIS BRDF product," *Int. J. Appl. Earth Obs. Geoinf.*, vol. 44, pp. 53-60, 2016-01-01. 2016, doi: 10.1016/j.jag.2015.07.007.

[25] G. Zhu, W. Ju, J. M. Chen, P. Gong, B. Xing, and J. Zhu, "Foliage Clumping Index Over China's Landmass Retrieved From the MODIS BRDF Parameters Product," *IEEE Trans. Geosci. Remote Sensing*, vol. 50, no. 6, pp. 2122-2137. 2012, doi: 10.1109/TGRS.2011.2172213.

[26] J. Pisek, J. M. Chen, and T. Nilson, "Estimation of vegetation clumping index using MODIS BRDF data," *Int. J. Remote Sens.*, vol. 32, no. 9, pp. 2645-2657. 2011.

[27] X. R. Xu, W. J. Fan, J. C. Li, P. Zhao, and G. X. Chen, "A unified model of bidirectional reflectance distribution

function for the vegetation canopy," *Science China Earth Sciences*, vol. 60, no. 3, pp. 463-477. 2017.

[28] X. Li, A. H. Strahler, and C. E. Woodcock, "A hybrid geometric optical-radiative transfer approach for modeling albedo and directional reflectance of discontinuous canopies," *Geoscience and Remote Sensing, IEEE Transactions on*, vol. 33, no. 2, pp. 466-480. 1995.

[29] W. Fan, J. Li, and Q. Liu, "GOST2: The Improvement of the Canopy Reflectance Model GOST in Separating the Sunlit and Shaded Leaves," *IEEE J. Sel. Top. Appl. Earth Observ. Remote Sens.*, vol. 8, no. 4, pp. 1423-1431. 2015, doi: 10.1109/JSTARS.2015.2413994.

[30] S. Wu *et al.*, "Modeling Discrete Forest Anisotropic Reflectance Over a Sloped Surface With an Extended GOMS and SAIL Model," *IEEE Trans. Geosci. Remote Sensing*, vol. 57, no. 2, pp. 944-957. 2019, doi: 10.1109/TGRS.2018.2863605.

[31] T. Nilson, "Inversion of gap frequency data in forest stands," *Agric. For. Meteorol.*, vol. 98-9, no. SI, pp. 437-448. 1999.

[32] J. M. Chen and S. G. Leblanc, "A four-scale bidirectional reflectance model based on canopy architecture," *Geoscience and Remote Sensing, IEEE Transactions on*, vol. 35, no. 5, pp. 1316-1337. 1997.

[33] J. Geng *et al.*, "GOFP: A Geometric-Optical Model for Forest Plantations," *IEEE Trans. Geosci. Remote Sensing*, vol. 55, no. 9, pp. 5230-5241. 2017, doi: 10.1109/TGRS.2017.2704079.

[34] J. Geng *et al.*, "Influence of the exclusion distance among trees on gap fraction and foliage clumping index of forest plantations," *Trees*, vol. 30, no. 5, pp. 1683-1693. 2016, doi: 10.1007/s00468-016-1400-y.

[35] W. Fan, J. M. Chen, W. Ju, and G. Zhu, "GOST: A Geometric-Optical Model for Sloping Terrains," *IEEE Trans. Geosci. Remote Sensing*, vol. 52, no. 9, pp. 5469-5482. 2014, doi: 10.1109/TGRS.2013.2289852.

[36] T. Nilson and U. Peterson, "A forest canopy reflectance model and a test case," *Remote Sens. Environ.*, vol. 37, no. 2, pp. 131-142. 1991, doi: 10.1016/0034-4257(91)90024-Z.

[37] A. Kuusk, T. Nilson, M. Paas, M. Lang, and J. Kuusk, "Validation of the forest radiative transfer model FRT," *Remote Sens. Environ.*, vol. 112, no. 1, pp. 51-58, 2008-01-15. 2008, doi: 10.1016/j.rse.2006.06.025.

[38] X. Xu, W. Fan, J. Li, P. Zhao, and G. Chen, "A unified model of bidirectional reflectance distribution function for the vegetation canopy," *Science China Earth Sciences*, vol. 60, no. 3, pp. 463-477. 2017, doi: 10.1007/s11430-016-5082-6.

[39] J. Geng, J. M. Chen, and L. Tu, "Application of a Hypergeometric Model in Simulating Canopy Gap Fraction and BRF for Forest Plantations on Sloping Terrains," *IEEE J. Sel. Top. Appl. Earth Observ. Remote Sens.*, p. 1. 2022, doi: 10.1109/JSTARS.2022.3156403.

[40] D. Wit, "Photosynthesis of Leaf Canopies,". 1965.

[41] W. Verhoef, "Theory of radiative transfermodels applied in optical remote sensing of vegetation canopies,", 1998.

[42] B. M. P. G. Graham Russell, *Plant Canopies: Their Growth, Form and Function*: Cambridge University Press, 1990.

[43] J. Pisek, O. Sonnentag, A. D. Richardson, and M. Mõttus, "Is the spherical leaf inclination angle distribution a valid assumption for temperate and boreal broadleaf tree species?" *Agric. For. Meteorol.*, vol. 169, pp. 186-194. 2013, doi: 10.1016/j.agrformet.2012.10.011.

[44] W. Verhoef, "Light scattering by leaf layers with application to canopy reflectance modeling: The SAIL model," *Remote Sens. Environ.*, vol. 16, no. 2, pp. 125-141, 1984-10-01. 1984, doi: 10.1016/0034-4257(84)90057-9.

[45] J. Geng *et al.*, "Error Analysis of LAI Measurements with LAI-2000 Due to Discrete View Angular Range Angles for Continuous Canopies," *Remote Sens.*, vol. 13, no. 7, p. 1405, 2021-04-06. 2021, doi: 10.3390/rs13071405.

[46] X. Li and A. H. Strahler, "Modeling the gap probability of a discontinuous vegetation canopy," *Geoscience and Remote Sensing, IEEE Transactions on*, vol. 26, no. 2, pp. 161-170. 1988.

[47] S. G. Leblanc, J. M. Chen, R. Fernandes, D. W. Deering, and A. Conley, "Methodology comparison for canopy structure parameters extraction from digital hemispherical photography in boreal forests," *Agric. For. Meteorol.*, vol. 129, no. 3, pp. 187-207. 2005.

[48] G. Yin *et al.*, "Path Length Correction for Improving Leaf Area Index Measurements Over Sloping Terrains: A Deep Analysis Through Computer Simulation," *IEEE Trans. Geosci. Remote Sensing*, vol. 58, no. 7, pp. 4573-4589. 2020, doi: 10.1109/TGRS.2019.2963366.

[49] J. Qi *et al.*, "LESS: LargE-Scale remote sensing data and image simulation framework over heterogeneous 3D scenes," *Remote Sens. Environ.*, vol. 221, pp. 695-706. 2019, doi: 10.1016/j.rse.2018.11.036.

[50] A. Gonsamo, J. N. Walter, and P. Pellikka, "CIMES: A package of programs for determining canopy geometry and solar radiation regimes through hemispherical photographs," *Comput. Electron. Agric.*, vol. 79, no. 2, pp. 207-215, 2011-01-01. 2011, doi: https://doi.org/10.1016/j.compag.2011.10.001.